ISSN (Print) 1226-1750
ISSN (Online) 2233-6656
Journal of Magnetics 27(4), 341-346 (2022) https://doi.org/10.4283/JMAG.2022.27.4.341

Temperature-dependent Scaling Behavior of Magnetic Hysteresis Loop of CoFeB/Pd Multilayer Film

Nguyen Le Thi[1,2], Anabil Gayen[1], Yunxiu Zhao[1], Jae-Hyun Ha[3], Jung-Il Hong[3], and Dong-Hyun Kim[1]*

[1]Department of Physics, Chungbuk National University, Cheongju 28644, Republic of Korea
[2]Hong Duc University, Thanh Hoa City, Vietnam
[3]Department of Physics and Chemistry, DGIST, Daegu 42988, Republic of Korea

(Received 30 September 2022, Received in final form 1 December 2022, Accepted 5 December 2022)

We report our experimental investigation on the temperature-dependent hysteresis loops and magnetic domain behaviors of CoFeB (0.4 nm)/Pd (1 nm) multilayer on polyimide substrate with a perpendicular magnetic anisotropy, by means of magneto-optical Kerr microscopy. Hysteresis characteristics such as saturation magnetization, coercivity, and hysteresis loop area with respect to the temperature have been analyzed, where power-law scaling behaviors are observed with microscopic magnetic domain patterns mediated by numerous nucleation sites.

Keywords : scaling behavior, hysteresis loop, magnetic domains, CoFeB/Pd multilayer, polyimide substrate

1. Introduction

Ferromagnetic multilayer films with a perpendicular magnetic anisotropy (PMA) have been of immense interest thanks to many promising properties as well as applicability in spintronics. For instance, CoFeB/Pd films are known to exhibit high spin polarization [1], amorphous ferromagnetic film structure [2], and strong perpendicular magnetic anisotropy [3]. Recently, numerous studies on modification and control of magnetic properties for the multilayer films have been conducted on flexible substrates [4-12]. For magnetic films on flexible substrates, thermal and structural stability of flexible substrates are required, since magnetic films on flexible substrates may be subject to thermal and, particularly, structural stresses. Considering the above factors, polyimide (PI) is widely used for flexible substrates for magnetic films [13-15].

On the other hand, magnetic hysteresis behavior is considered to be one of most important and urgent magnetic properties when every magnetic sample is prepared. The ferromagnetic hysteresis curve is known to be intrinsically dependent on the temperature due to the competition between thermal agitation and magnetic ordering [16]. Numerous studies have been devoted to hysteresis loops and the magnetic domain structure of thin film fabricated on conventional rigid substrates [17, 18]. However, relatively very few studies have been devoted to the temperature-dependent hysteresis behavior for the film prepared on non-rigid substrate such as PI. Considering that the elastic deformation of the sample [19-21] arising from the thermal expansion mismatch between the film and the substrate, magnetic properties could be complicated under temperature variation due to the different thermal expansion properties. Compared to films grown on conventional rigid substrates, magnetic thin films grown on flexible substrates exhibit distinctive magnetic properties such as magnetoelastic coupling, magnetoresistance [22], and spin reorientation behavior [23]. Thus, temperature-dependent magnetic properties such as hysteresis loop behavior for the films fabricated on flexible substrate could provide meaningful information for better understanding of temperature-dependent feature of ferromagnetic samples.

In this work, we report our experimental investigation on the temperature-dependent hysteresis behavior of CoFeB/Pd multilayer film with perpendicular magnetic anisotropy prepared on PI substrate with direct observation of magnetic domain patterns by means of magneto-optical Kerr microscopy, where power-law scaling behaviors are observed for the saturation magnetization, the coercivity,

*Corresponding author: Tel: +82-43-261-2268
Fax: +82-43-274-7811, e-mail: donghyun@chungbuk.ac.kr

and the area of the hysteresis loops.

2. Experimental

The ferromagnetic thin film of Ta (3 nm)/Pt (3 nm)/ $Co_{40}Fe_{40}B_{20}$ (0.4 nm)/Pd (1 nm)/Ta (2 nm) multilayer with a perpendicular magnetic anisotropy was deposited on 50 μm thick PI substrate by a DC magnetron sputtering. Commercially available PI (Kapton® from Dupont) was used for substrates. The nominal composition of the CoFeB was selected to be 40:40:20, as this composition exhibits a substantial spin polarization as reported in Ref. [1]. The buffer layer Ta (3 nm)/Pt (3 nm) was used for better adhesion and good surface morphology. A 2-nm thick Ta layer was deposited on the sample as a capping layer to prevent oxidation. Before deposition, PI substrate was cleaned in ethanol for 5 minutes by ultrasonic washing machine. During the sputtering procedure, Ar pressure within the chamber was maintained at 2.0 mTorr. The saturation magnetization M_S = 458 ± 12 emu/cc at room temperature, which was measured by vibrating sample magnetometer. The hysteresis behaviour and domain pattern of CoFeB/Pd multilayer film was observed at temperature range of 210 K to 330 K with step of 10 K by using polar magneto-optical Kerr effect (MOKE) microscopy with a cryostat for a sample area of 256 × 192 μm^2.

3. Results and Discussion

Hysteresis loops of CoFeB/Pd multilayer film grown on PI substrate were measured in the polar MOKE geometry at different temperatures. The selected MOKE hysteresis loops have been plotted in Fig. 1. Hysteresis loops along perpendicular direction are clearly observed at low temperatures, whereas the loop becomes narrower and slanted with increasing temperature. Note that the hysteresis loops are normalized by the saturation magnetization at 210 K. Squareness of the hysteresis loop (M_r/M_S) is close to 1 below 260 K and decreases from ~0.8 at 260 K to ~0.1 at 320 K, where M_r is the remanent magnetization and M_S is the saturation magnetization. As the temperature increases and approaches near the Curie temperature, the slopes of the hysteresis loops gradually become flatten, as in the case of 330 K, implying that the film becomes paramagnetic.

The saturation magnetization normalized by the saturation magnetization at 210 K with respect to the temperature is shown in Fig. 2. The saturation magnetization decreases with respect to the temperature, where the measured data is fitted by the power law:

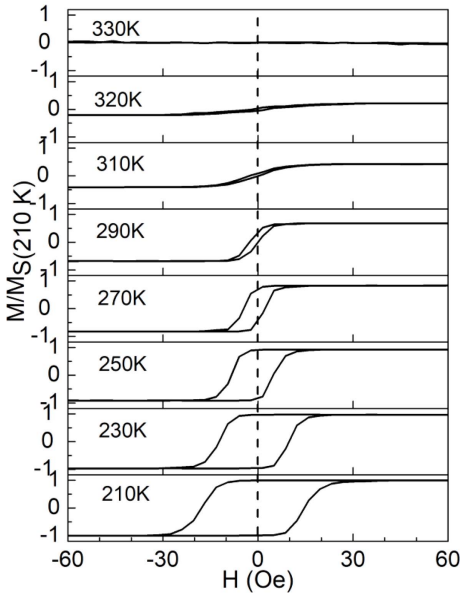

Fig. 1. Selected hysteresis loops of CoFeB/Pd multilayer film deposited on PI substrate at various temperatures with the direction of magnetic field perpendicular to the film plane.

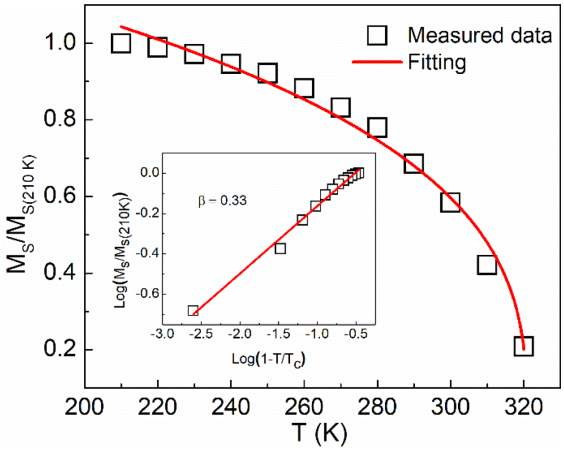

Fig. 2. (Color online) The saturation magnetization normalized by the saturation magnetization at 210 K with respect to the temperature. The solid line is the fitting curve of power law for the saturation magnetization. Inset is a log-log plot of the magnetization as a function of temperature for T_C = 320.8 K. The slope of the straight line gives the power-law exponent β = 0.33.

$\frac{M_S(T)}{M_{S(210\,K)}} = \frac{M_S(0)}{M_{S(210\,K)}}\left(1-\frac{T}{T_C}\right)^{\beta}$ [24-27]. $\frac{M_S(0)}{M_{S(210\,K)}}$ is fitted to be 1.48 and T_C to be about 320.8 K. The power-law exponent β is found to be about 0.33. Inset figure is a log-log plot of the figure with the exponent β = 0.33. The β value is close to the prediction from the 3D Heisenberg model (β = 0.37) [24] and also consistent with the

reported values in [26, 27]. Observed β value is far from the prediction based on the 2D Ising model (0.125) and 2D XY (0.23) model [24], implying the continuous variation of magnetization around the Curie temperature rather than behavior with Ising-like discreteness. The Curie temperature (T_C = 320.8 K) observed in the present film sample prepared on PI is closer to room temperature, significantly lower than the T_C value (~453 K) reported for films on rigid substrate [28], which could be originated from the thermal expansion mismatch between the substrate and the film. Since the thermal expansion coefficient of the PI (20 × 10^{-6} K^{-1}) [29] is larger than that of the silicon (2.56 × 10^{-6} K^{-1}) [30], the larger lattice mismatch between the PI substrate and the film, compared to the case of Si substrates, might result in the reduced Curie temperature. Moreover, the roughness of PI substrate (2.8 nm) is larger than that of Si substrates (0.431 nm) [12], which also might effectively reduce the Curie temperature.

The coercivity determined from the hysteresis loop at different temperatures is shown in Fig. 3. Apparently, the coercivity decreases monotonically with increasing temperature. Temperature-dependent coercivities are well fitted with the power-law model: $H_C(T) = H_0(0)(1\text{-}T/T_B)^{\alpha}$ [31, 32]. $H_0(0)$ was 125.8 Oe, the blocking temperature (T_B) is 316.6 K, which is close to the Tc value but slightly less. This might be from the granular film structure on PI [33, 34]. The inset is the log-log plot of H_C versus (1-T/T_B) with the exponent value of α = 1.62. The exponent value obtained in the current system is much larger than what is fitted by a simple model such as Kneller's law

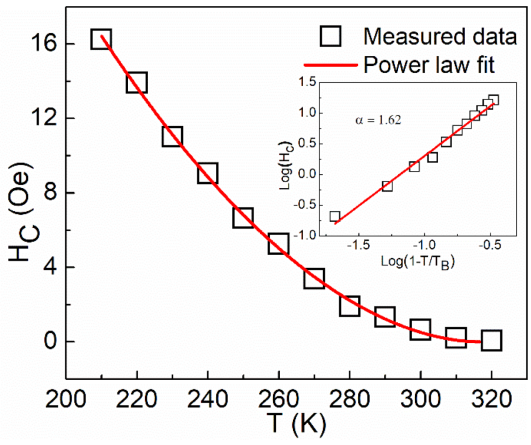

Fig. 3. (Color online) Dependence of coercivity on temperature for CoFeB/Pd multilayer film. The solid line displays the fitted curve according to the power-law model ($H_C(T) = H_0(0)(1\text{-}T/T_B)^{\alpha}$). The inset is log-log of H_C vs 1-T/T_B. The slope of the straight line corresponds to the exponent value α = 1.62.

[35]. Since our temperature region is above 210 K, which is not far away from the critical temperature, the exact exponent value should be rechecked down to 4 K, which is not allowed by the present setup. However, at least, we can state that the coercivity scaling does not follow a conventional Kneller-type exponent observed so far for ferromagnetic films on rigid substrate. We consider that this could be due to the scaling behavior in a cut-off region near the critical temperature, or the reversal statistics is quite different from the amorphous nature of CoFeB film [36]. Moreover, CoFeB is known to have a positive magnetostriction coefficient [37]. Thus, there exists a magnetostriction, however, there also exist substantial number of defects potentially modifying the magnetic anisotropy [12, 38, 39] and trapping magnetic domain walls, leading to a different coercivity scaling exponent.

To further understand the hysteresis behavior of the ferromagnetic system, the temperature dependent-scaling behavior of the hysteresis area has been investigated. The relationship between the dynamic loop area and the external parameters such as temperature (T), amplitude (H_0), and frequency (ω) is expressed as the Steinmetz law: $A\text{-}A_0 \propto H_0^{\alpha}\omega^{\beta}T^{-\gamma}$ [40], A_0 is the zero-frequency loop area. In the present study, the field sweep rate (hence frequency) and the maximum applied field were kept constant, only observing γ from the temperature-dependent hysteresis loop area. Fig. 4 shows the observed hysteresis loop area as a function of temperature. The hysteresis loop area decreases as the temperature increases due to the decrease in magnetization and coercivity with increasing temperature. The inset shows the log-log plot of area vs. temperature. It can be found

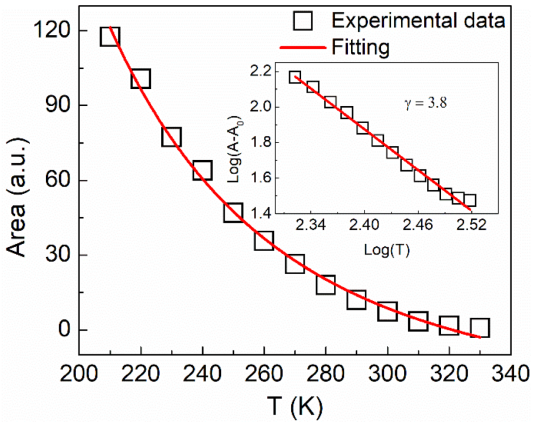

Fig. 4. (Color online) The typical hysteresis loop area with respect to the temperature. The inset is a log-log plot of hysteresis loop area to the temperature. The loop area follows the straight line, providing a scaling exponent of γ = 3.8.

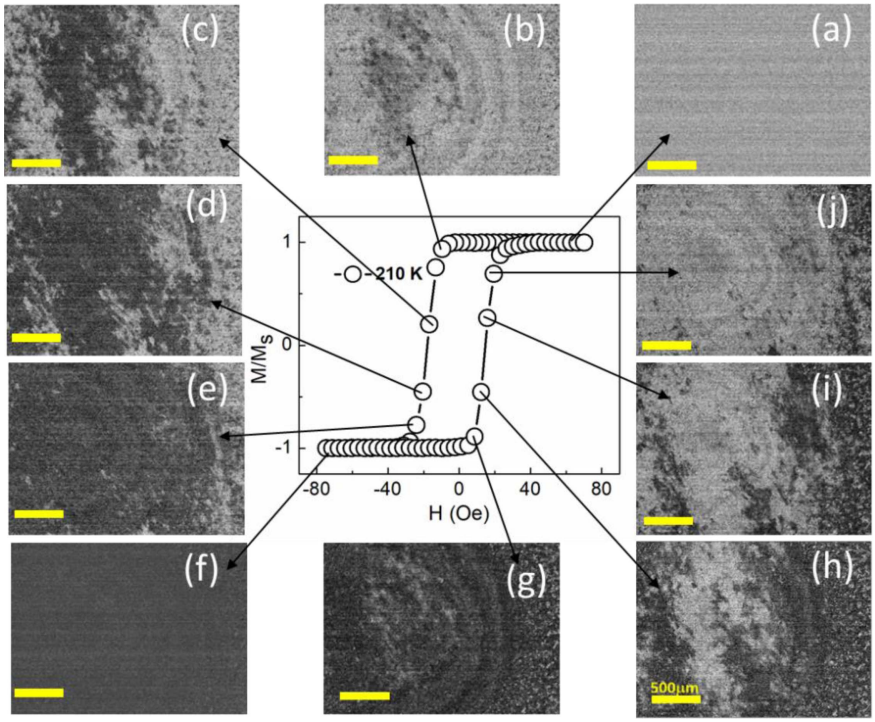

Fig. 5. (Color online) Magnetization-reversal process in sample CoFeB/Pd observed by polar Kerr microscopy at 210 K. All domain images have scale bars corresponding to 500 μm.

that the value of Log(A-A_0) decreases linearly with the increase of Log(T), which exhibits a scaling behavior of area (A-A_0) $\alpha\ T^{-\gamma}$. From the fitting of the slope, the value of the loop area scaling exponent $\gamma = 3.8$. The measured value in the present study is considerably higher compared to the a few reports available till date [40, 41]. As in the case of coercivity scaling, discussed above, the discrepancy is considered to probably arise from different magnetization reversal processes observed in magnetic film on PI [41, 42], possibly having more defects and intrinsic magnetostriction effect [43-47].

In order to examine the magnetization reversal behavior of CoFeB/Pd films on PI, magnetic domain behavior is observed simultaneously with hysteresis loop measurements using polar MOKE with a cryostat. Fig. 5 displays the domain patterns of the film at the selected temperature of 210 K. Fig. 5(a) is the initial magnetic domain without state switching at a positive saturation magnetic field of 80 Oe. The reversal process starts with nucleation at a negative field of -8 Oe (Fig. 5(b)). The black (white) domains correspond to the down (up) magnetization. The magnetic domains rapidly increase in size due to the propagation speed of the domain wall, as shown in Figs. 5(c)-(e), when the black regions dominate the entire thin film, the magnetization reversal is almost complete (Fig. 5(f)). The process of reversing the magnetization from a negative field direction to a positive field direction is also performed similarly, as indicated by the contrasting evolution of the white domains, as shown in Figs. 5(g)-(j). The overall domain patterns are observed to be statistically symmetric.

The evolution of the domain pattern in the same area was observed at various temperatures as shown in Fig. 6, these domains were recorded at a magnetic field close to the coercivity. The contrast of magnetic domains become more vacant as the temperature increases, approaching the Curie temperature. At relatively higher temperatures, the domains are observed to be quite mobile and faster, as the magnetization can be more easily reversed with the help of thermal agitation. Overall, the domain patterns are quite complex, unlike the sample prepared on rigid substrates.

4. Conclusions

We have fabricated CoFeB/Pd multilayer films with PMA on flexible PI substrate. Magnetic domain patterns and corresponding hysteresis loops are systematically measured with variation of temperatures using the MOKE microscopy. The temperature-dependent magnetization exhibits a scaling behavior with the exponent matching with 3D Heisenberg model, while the scaling exponents

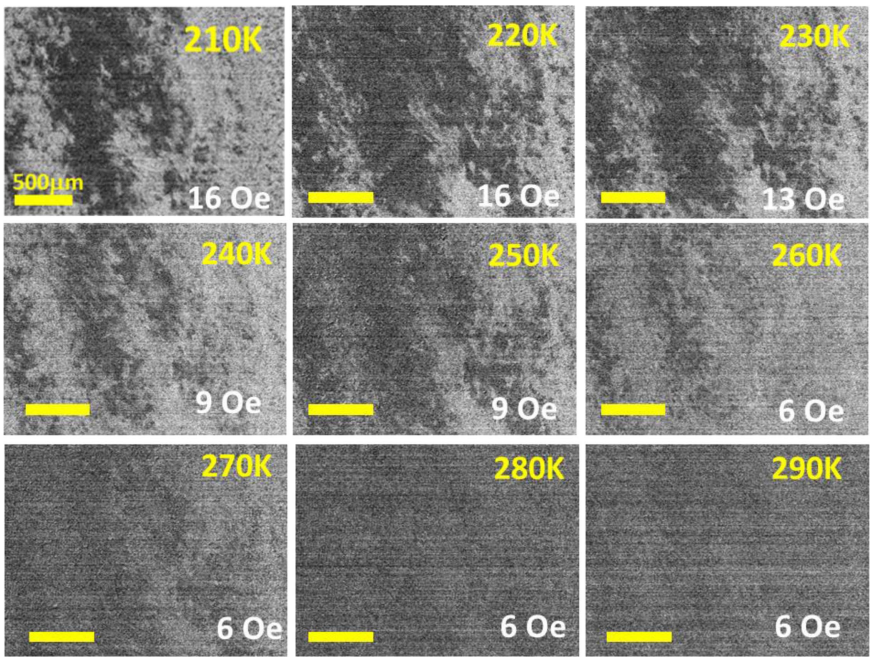

Fig. 6. (Color online) Magnetic domain images recorded near coercivity at different temperatures of CoFeB/Pd on PI substrate. A scale bar of 500 μm is used for all magnetic domain images.

of the coercivity and the loop area scaling are quite different from the reports observed for magnetic film on the rigid substrate. The corresponding magnetic domain is also observed to be nucleation-dominant with complex patterns, implying the different scaling behavior could exist for films in the present study. We believe that our work, temperature-dependent hysteresis scaling behavior for magnetic films on flexible substrate, may open up meaningful perspectives for the development of flexible electronic devices.

Acknowledgments

This research was supported by Chungbuk National University Korea National University Development Project (2020).

References

[1] S. X. Huang, T. Y. Chen, and C. L. Chien, Appl. Phys. Lett. **92**, 242509 (2008).
[2] C. Fowley, N. Decorde, K. Oguz, K. Rode, H. Kurt, and J. M. D. Coey, IEEE Trans. Magn. **46**, 2116 (2010).
[3] J. H. Jung, S. H. Lim, and S. R. Lee, Appl. Phys. Lett. **96**, 042503 (2010).
[4] J. Liu, J. Chen, Y. Zhang, S. Fu, G. Chai, C. Cao, X. Zhu, Y. Guo, W. Cheng, D. Jiang, Z. Zhao, and Q. Zhan, ACS Appl. Mater. Interfaces **13**, 29975 (2021).
[5] M. Hassan, S. Laureti, C. Rinaldi, F. Fagiani, S. Varotto, G. Barucca, N. Y. Schmidt, G. Varvaro, and M. Albrecht, Nanoscale Adv. **3**, 3076 (2021).
[6] H. Li, Y. Ma, and Y. Huang, Mater. Horiz. **8**, 383 (2021).
[7] I. Fina, N. Dix, E. Menéndez, A. Crespi, M. Foerster, L. Aballe, F. Sánchez, and J. Fontcuberta, ACS Appl. Mater. Interfaces **12**, 15389 (2020).
[8] E. Pandey, B. B. Singh, P. Sharangi, and S. Bedanta, Nano Ex. **1**, 010037 (2020).
[9] S. Ota, T. Hirai, K. Ochi, T. Namazu, T. Ina, T. Koyama, and D. Chiba, J. Appl. Phys. **127**, 173901 (2020).
[10] M. Belusky, S. Lepadatu, J. Naylor, and M. M. Vopson, J. Magn. Magn. Mater. **478**, 77 (2019).
[11] J.-H. Kwon, W.-Y. Kwak, and B. K. Cho, Sci. Rep. **8**, 1 (2018).
[12] T. Vemulkar, R. Mansell, A. Fernández-Pacheco, and R. P. Cowburn, Adv. Funct. Mater. **26**, 4704 (2016).
[13] P. Taptimthong, J. Rittinger, M. C. Wurz, and L. Rissing, Procedia Technology **15**, 230 (2014).
[14] M. Z. Pakhuruddin, K. Ibrahim, and A. Abdul Aziz, J. Optoelectron. Adv. Mater. **7**, 377 (2013).
[15] B. Ma, J. Ren, J. Deng, and W. Yuan, 2010 IEEE 23rd International Conference on Micro Electromechanical Systems (MEMS). IEEE, 679, (2010).
[16] G. Bertotti, Hysteresis in magnetism: for physicists, materials scientists, and engineers. Gulf Professional Publishing, (1998).
[17] D.-T. Ngo, D.-T. Quach, Q.-H. Tran, K. Møhave, T.-L. Phan, and D.-H. Kim, J. Phys. D: Appl. Phys. **47**, 445001 (2014).
[18] J. H. Jung, B. Jeong, S. H. Lim, and S.-R. Lee, Appl.

Phys. Express **3**, 023001 (2010).
[19] V. M. Marx, F. Toth, A. Wiesinger, J. Berger, C. Kirchlechner, M. J. Cordill, F. D. Fischer, F. G. Rammerstorfer, and G. Dehm, Acta Mater. **89**, 278 (2015).
[20] J. Luo, Y. Sun, B. Wang, Z. Jin, S. Yang, Y. Wang, and G. Ding, AIP Adv. **8**, 115134 (2018).
[21] Y. Y. Hu and W. M. Huang, Handbook of Manufacturing Engineering and Technology, Springer-Verlag, London (2015).
[22] J. Rittinger, P. Taptimthong, L. Jogschies, M. C. Wurz, and L. Rissing, Smart Sensors, Actuators, and MEMS VII; and Cyber Physical Systems. **9517**, SPIE (2015).
[23] K. S. Maneesh, J. Arout Chelvane, A. Talapatra, H. Basumatary, J. Mohanty, and S. V. Kamat, J. Magn. Magn. Mater. **448**, 31 (2018).
[24] F. Huang, M. T. Kief, G. J. Mankey, and R. F. Willis, Phys. Rev. B **49**, 3962 (1994).
[25] M. Farle, W. A. Lewis, and K. Baberschke, Appl. Phys. Lett. **62**, 2728 (1993).
[26] Z. Y. Liu, G. H. Yu, and Z. C. Wang, Phys. Rev. B **72**, 064451 (2005).
[27] L. Li, D. Han, W. Lei, Z. Liu, F. Zhang, X. Mao, P. Wang, and H. Hou, J. Appl. Phys. **116**, 123904 (2014).
[28] D.-T. Quach, T.-D. Chu, D.-T. Ngo, and D.-H. Kim, Phys. B: Condens. Matter **577**, 411822 (2020).
[29] DuPont™ Kapton® 200EN Polyimide Film. matweb.com.
[30] P. Becker, P. Scyfried, and H. Siegert, Z. Physik B Condensed Matter **48**, 1 (1982).
[31] E. F. Kneller and F. E. Luborsky, J. Appl. Phys. **34**, 656 (1963).
[32] K. Maaz, S. Karim, K. J. Lee, M.-H. Jung, and G.-H. Kim, Mater. Chem. Phys. **133**, 1006 (2012).
[33] F. F. Yang, S. S. Yan, M. X. Yu, S. S. Kang, Y. Y. Dai, Y. X. Chen, S. B. Pan, J. L. Zhang, H. L. Bai, D. P. Zhu, S. Z. Qiao, W. W. Pan, G. L. Liu, and L. M. Mei, J. Alloys Compd. **558**, 91 (2013).
[34] Y.-S, Hsiao, C.-P. Chen, C.-H. Chao, and W.-T. Whang, Org. Electron. **10**, 551 (2009).
[35] S. Ishrat, K. Maaz, K.-J. Lee, M.-H. Jung, and G.-H. Kim, J. Solid State Chem. **210**, 116 (2014).
[36] F. Liu, Z. Liu, S. Gao, Q. You, L. Zou, J. Chen, J. Liu, and X. Liu, RSC Adv. **8**, 19034 (2018).
[37] Y. Liu, B. Wang, Q. Zhan, Z. Tang, H. Yang, G. Liu, Z. Zuo, X. Zhang, Y. Xie, X. Zhu, B. Chen, J. Wang, and R.-W. Li, Sci. Rep **4**, 1 (2014).
[38] Y.-C. Hsieh and M. Mansuripur, J. Appl. Phys. **78**, 380 (1995).
[39] M. T. Rahman, N. N. Shams, Y.-C. Wu, and C.-H. Lai, Appl. Phys. Lett. **91**, 132505 (2007).
[40] Z. Huang, F. Zhang, Z. Chen, and Y. Du, Eur. Phys. J. B **44**, 423 (2005).
[41] B. C. Choi, W. Y. Lee, A. Samad, and J. A. C. Bland, Phys. Rev. B **60**, 11906 (1999).
[42] W. Y. Lee, B.-Ch. Choi, Y. B. Xu, and J. A. C. Bland, Phys. Rev. B **60**, 10216 (1999).
[43] N. N. Phuoc, L. T. Hung, and C. K. Ong, J. Phys. D: Appl. Phys. **43**, 255001 (2010).
[44] X. Qiao, B. Wang, Z. Tang, Y. Shen, H. Yang, J. Wang, Q. Zhan, S. Mao, X. Xu, and R.-W. Li, AIP Adv. **6**, 056106 (2016).
[45] M. Belusky, S. Lepadatu, J. Naylor, and M. M. Vopson, J. Magn. Magn. Mater. **478**, 77 (2019).
[46] C. Feng, Y. Li, L. Wang, Y. Cao, M. Yao, F. Meng, F. Yang, B. Li, K. Wang, and G. Yu, Adv. Funct. Mater. **30**, 1909708 (2020).
[47] Z. Tang, H. Ni, B. Lu, M. Zheng, Y.-A. Huang, S.-G. Lu, M. Tang, and J. Gao, J. Magn. Magn. Mater. **426**, 444 (2017).